*Journal of The Electrochemical Society*, **151** (7) G482-G487 (2004)
0013-4651/2004/151(7)/G482/6/$7.00 © The Electrochemical Society, Inc.

# Effect of Slurry Flow Rate on Tribological, Thermal, and Removal Rate Attributes of Copper CMP

**Z. Li,[a,*,z] L. Borucki,[b,**] I. Koshiyama,[c] and A. Philipossian[a,**]**

[a]*University of Arizona, Department of Chemical and Environmental Engineering, Tucson, Arizona 85721 USA*
[b]*Intelligent Planar, Mesa, Arizona 85205 USA*
[c]*Fujimi Incorporated, Kagamigahara, Gifu Prefecture 509-0108, Japan*

Chemical mechanical polishing of copper is examined experimentally and theoretically as a function of slurry flow rate and the product of applied wafer pressure and relative sliding speed ($p \times V$). It is observed that under constant tribological conditions, the removal rate at any fixed value of $p \times V$ generally decreases as slurry flow rate increases. The increased cooling of the wafer surface, as a result of increased slurry flow rate, is used to explain this reduction in the reaction rate. At a fixed flow rate, it is further observed that removal rate does not necessarily increase monotonically with $p \times V$. The rate instead depends on the particular values of pressure and velocity, regardless of the fact that they may result in the same value of $p \times V$. This dependence is shown to be caused by changes in the coefficient for convective heat-transfer between the wafer and the slurry, as well as the heat partition factor, which determines the fraction of the total frictional power that heats the wafer. Results further indicate that trends in copper removal rate can be adequately explained with a Langmuir-Hinshelwood kinetics model with both mechanical and chemical rate components.
 [DOI: 10.1149/1.1758818] 

Manuscript submitted November 7, 2003; revised manuscript received January 3, 2004. Available electronically June 10, 2004.

Copper polishing in rotary chemical mechanical planarization (CMP) tools is an important step in the production of copper interconnects using the dual-damascene process. It has been observed that the polish rate of copper is highly sensitive to temperature, with an activation energy on the order of 0.5-0.6 eV.[1,2] This indicates that a 10°C change in the temperature of the pad may be sufficient to double the copper removal rate.[2] Because of this sensitivity, the rate and uniformity of copper polishing can be affected by factors that by intent or by accident change the thermal environment of the wafer. Among the important recognized factors are the applied pressure $p$, the relative sliding velocity ($V$) between the wafer and the pad, and the kinetic coefficient of friction (COF) $\mu_k(t)$ that is interpolated linearly from COF data. The product $\mu_k(t)pV$ is the total power per unit area dissipated by friction by the wafer, pad, and slurry. Less well recognized is that this power may be partitioned unequally, providing more or less heating of the wafer depending on the particular conditions of sliding as well as the thermal conductivities of the materials involved.[3] Because heat loss is part of the energy balance for the wafer, factors that alter wafer cooling are also important. In particular, it is shown that increasing the slurry flow rate can lower the wafer temperature and reduce removal rate. Similarly, at a fixed power input, increasing the sliding speed can also reduce the polish rate through increased convective cooling of the wafer. All these effects can occur under otherwise constant tribological conditions, and large differences in rate are possible at constant values of $p \times V$.

## Experimental

Experiments were performed on a scaled version of a Speedfam-IPEC 472 polisher using Rodel's IC-1000 k-groove pads and Fujimi's PL-7102 copper slurry containing hydrogen peroxide as the oxidant. To measure the shear force between the pad and the wafer during polish, a sliding table was placed beneath the polisher. The sliding table consists of a bottom and a top plate that the polisher is set upon. As the wafer and pad are engaged, the top plate slides with respect to the bottom plate in only one direction due to friction between the pad and wafer. The degree of sliding is quantified by coupling the two plates to a load cell. The load cell is attached to a strain gauge amplifier that sends a voltage to a data acquisition board. The apparatus was calibrated to report the force associated with a particular voltage reading. Details of the experimental apparatus are described elsewhere.[4] Copper disks, having a nominal diameter of 100 mm and a purity of 99.99% were used as substrates. Previous studies[5] had shown that copper disks were a viable alternative to copper-deposited silicon wafers for tribological, thermal, and kinetic investigations. Conditioning was performed *in situ* using a diamond conditioner at a nominal applied pressure of 0.5 psi, rotational velocity of 30 rpm, and sweep frequency of 20 per min. Pad conditioning was followed by a 5 min pad break-in. Pressures and relative pad-wafer velocities were 1.5, 2.0, and 2.5 psi and 0.31, 0.62, and 1.09 m/s (40, 80, and 140 rpm), respectively. Slurry flow rates were 80 and 140 cc/min. These corresponded to flow rates of 215 and 377 cc/min on the 200 mm industrial Speedfam-IPEC 472 polisher. An infrared video camera was used to record pad temperatures at 0.2 s intervals at ten fixed locations near the pad at the leading edge. Real-time COF data were taken simultaneously along real-time infrared thermal measurements. Removal rates were calculated by determining the weight of the copper disk prior to and after polishing using a precise balance with a readability of 0.01 mg.

## Results

Figure 1 shows the Stribeck curves associated with the two flow rates. Over the range of Sommerfeld numbers considered, both Stribeck curves have slopes that are nearly zero. This implies that the tribological (wear) mechanism across the range of Sommerfeld

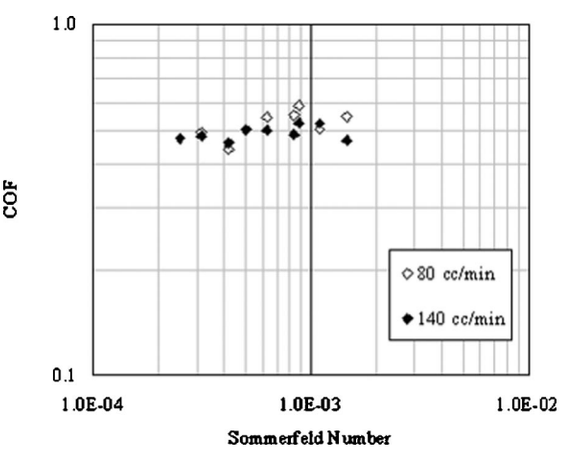


**Figure 1.** Stribeck curves at two slurry flow rates.

* Electrochemical Society Student Member.
** Electrochemical Society Active Member.
z E-mail: zhonglin@email.arizona.edu

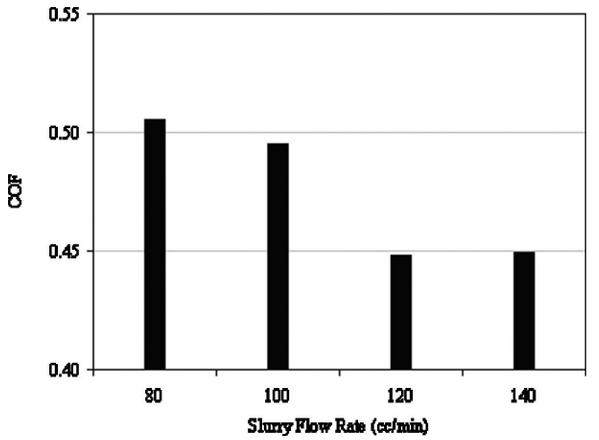


**Figure 2.** COF data at different flow rates (2.0 psi, 1.09 m/s).

numbers investigated is the same in both cases. The mean COF at 80 cc/min is 0.517, while at 140 cc/min, it is only slightly lower at 0.491. COFs of this magnitude, coupled with the relatively flat shape of the Stribeck curves, indicate the tribological mechanism to be that of "boundary lubrication" in which abrasive particles, pad asperities, and the surface of the wafer are all in direct contact with one another.

Figure 2 shows that at a constant wafer pressure and relative pad-wafer velocity, increasing the slurry flow rate from 80 to 140 cc/min reduces COF. This observation, coupled with the fact that slurry flow rate does not affect the lubrication mechanism, is significant because it shows that slurry flow rate can be used to modulate average COF without changing the lubrication mechanism. This is the key to isolating and studying the effect of COF on removal rate without having to worry about potential changes in the lubrication characteristics of the process with changes in flow rate.

Throughout the course of this study, removal rate data is represented in two ways. First, as in the case of Fig. 3, removal rate is plotted as a function of $p \times V$. Results indicate that copper removal is faster at 80 compared to 140 cc/min. The increase in removal rate at the lower flow rate is as much as 15%. In Fig. 3, the three left-hand-most pairs of data points were taken at a relative pad-wafer velocity of 0.31 m/s. The middle three pairs corresponded to 0.62 m/s, while the three right-hand-most pairs of data points were taken at 1.09 m/s. The most intriguing feature of Fig. 3 occurs in the region corresponding to a $p \times V$ value of about 11,000 Pa m/s ($W/m^2$), which coincides with the transition from 2.5 psi and 0.62 m/s to 1.5 psi and 1.09 m/s. In this region, as indicated in Fig. 1, the tribological mechanism and the COF are also nearly constant, yet according to Fig. 3, there is a notable drop in the removal rate at the

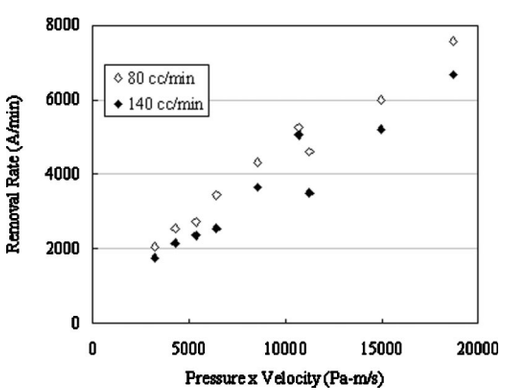


**Figure 3.** Removal rate as a function of $p \times V$ at two slurry flow rates.

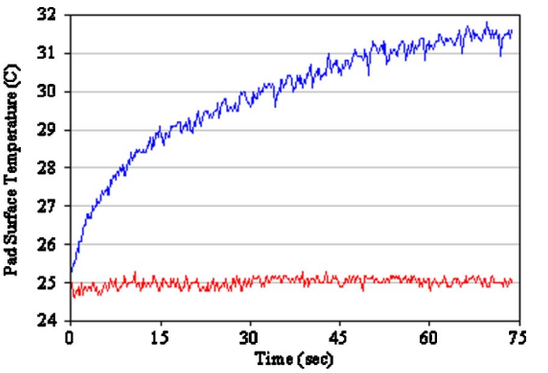


**Figure 4.** Comparison of temperature transients associated with (upper line) 2.5 psi and 1.09 m/s, and (lower line) 1.5 psi and 0.31 m/s.

higher velocity at both flow rates. This drop is more pronounced at higher flow rate. The reason for this observed non-Prestonian behavior is discussed later in this article by using appropriate thermal and reaction rate models.

The pad temperature transient measured by the IR camera corresponding to a slurry flow rate of 80 cc/min is shown in Fig. 4. Pad temperature transient for a given polishing run is defined as the difference between the average temperature of the pad at the end of the 75 s polishing interval and the average temperature of the pad at the beginning of the process. It can be seen that at the highest value of $p \times V$, the pad temperature increases by more than 6°C, while at the lowest value of $p \times V$, pad temperature remains nearly the same throughout the polish process. As a general trend, real-time thermal mapping of the pad surface indicated a rise in the average pad temperature with increasing values of $p \times V$.

Results show that pad temperature, slurry flow rate, and removal rate are all interrelated. In Fig. 5, removal rate data is plotted as a function of $1/k\overline{T}_p$, where $k$ is Boltzmann's constant and $\overline{T}_p$ is the mean pad temperature taken collectively over time at five sample points at the leading edge of the wafer. Again a reduction in removal rate is observed as flow rate is increased, and except at 1.09 m/s, the reduction in removal rate is actually associated with a slight increase in the mean leading edge pad temperature. Thus, the pad temperature is not necessarily a good indicator of the observed trends in removal rate. For a given slurry flow rate, the scatter in the data points shown in Fig. 5, as well as the apparent departure from a classical Arrhenius relationship (*i.e.*, the lack of a constant slope which would be indicative of the activation energy) is due to the

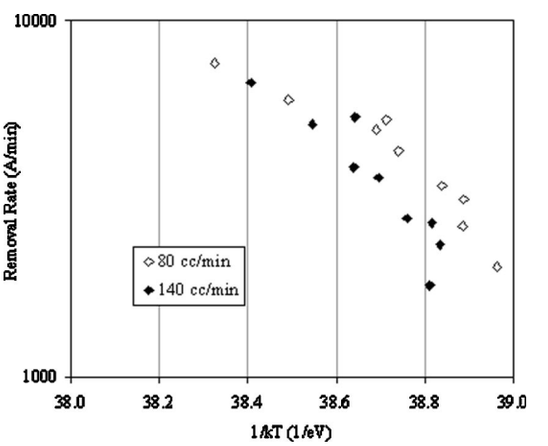


**Figure 5.** Removal rates *vs.* $1/kT$, where $T$ is the mean pad temperature at the leading edge of the wafer.

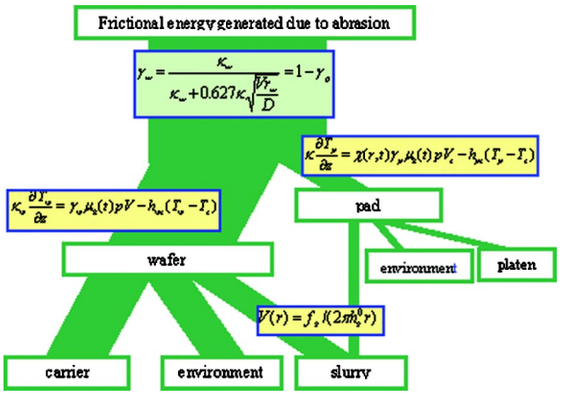


**Figure 6.** Thermal model and its associated energy balance.

dependence of removal rate on $1/kT$ (a thermal factor), as well as on $p \times V$ (a mechanical factor). In all cases the mean pad temperature is different from the mean wafer temperature, thus necessitating the construction of reliable thermal and reaction rate models in order to explain the observed trends in removal rate.

### Thermal and Reaction Rate Models

*Thermal model*.—Thermal analysis of the experimental data was performed with a model described in Ref. 6, in which the emphasis was on the thermal modeling of the pad. The schematic graph of the thermal model and its associated overall energy balance is shown in

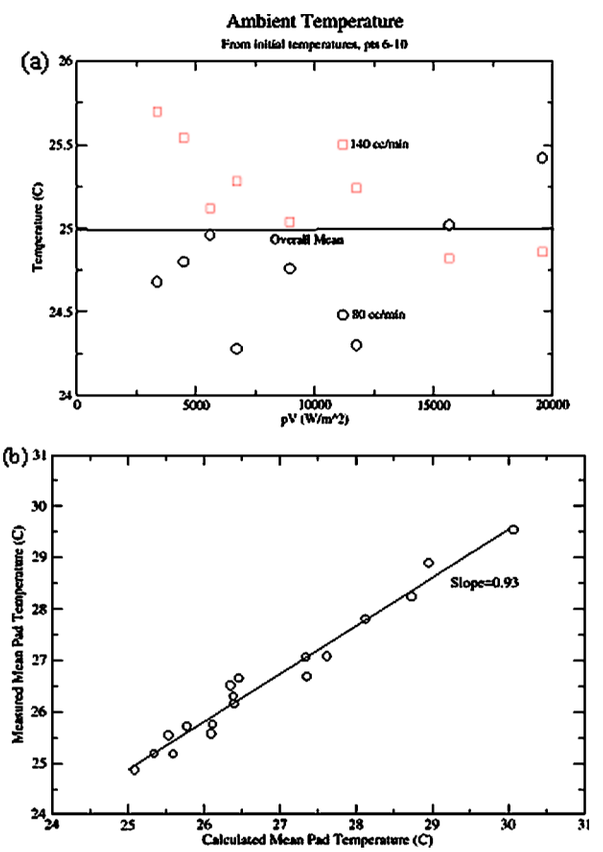


**Figure 7.** (a) Ambient temperatures estimated from IR thermal measurements. (b) Comparison of calculated and measured mean pad temperatures near the leading edge of the wafer.

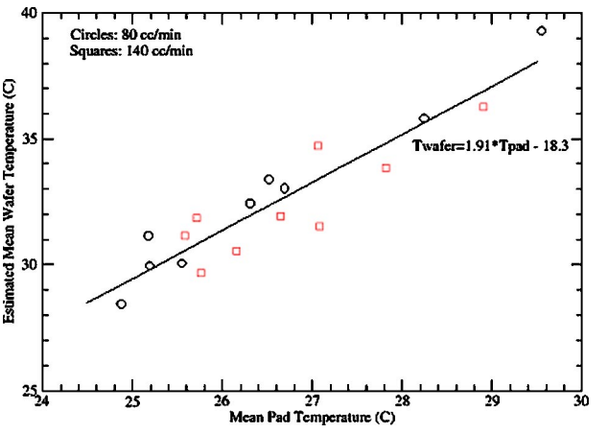


**Figure 8.** Estimated mean wafer temperatures corresponding to (○) 80 and (□) 140 cc/min.

Fig. 6. Focusing on the wafer, the heat flux $\mu_k(t)pV$ due to friction is partitioned between the wafer and pad with the fraction

$$\gamma_w = \frac{\kappa_w}{\kappa_w + 0.627\kappa\sqrt{\frac{Vr_w}{D}}} \quad [1]$$

entering the wafer.[3] In Eq. 1, $\kappa_w$ is an effective thermal conductivity associated with the wafer (which may depend on the surface layers present), $\kappa$ and $D$ are the thermal conductivity and thermal diffusivity of the pad, respectively, $V$ is the relative sliding speed, and $r_w$ is the wafer radius. The heat flux into the wafer is

$$\kappa_w\frac{\partial T_w}{\partial z} = \gamma_w\mu_k(t)pV - h_{ws}(T_w - T_s) \quad [2]$$

where $T_w$ is the local wafer temperature, $T_s$ is the local slurry temperature, and $h_{ws}$ is a heat-transfer coefficient for exchange between the wafer and slurry. From Eq. 1 and 2, it may be seen that an increase in the sliding speed $V$ results in a decrease in the heat partition fraction and therefore a decline in the fraction of the total heat flux to the wafer. The slurry temperature field $T_s$ in Eq. 2 is determined by the general model described in Ref. 6. In this model, the slurry exchanges heat with the pad, wafer, and air and convects it radially outward from the center of the pad with velocity

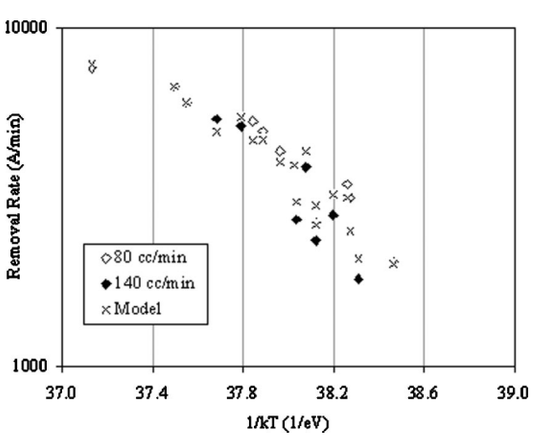


**Figure 9.** Removal rates *vs.* $1/kT$, where $T$ is the mean pad temperature at the leading edge of the wafer.

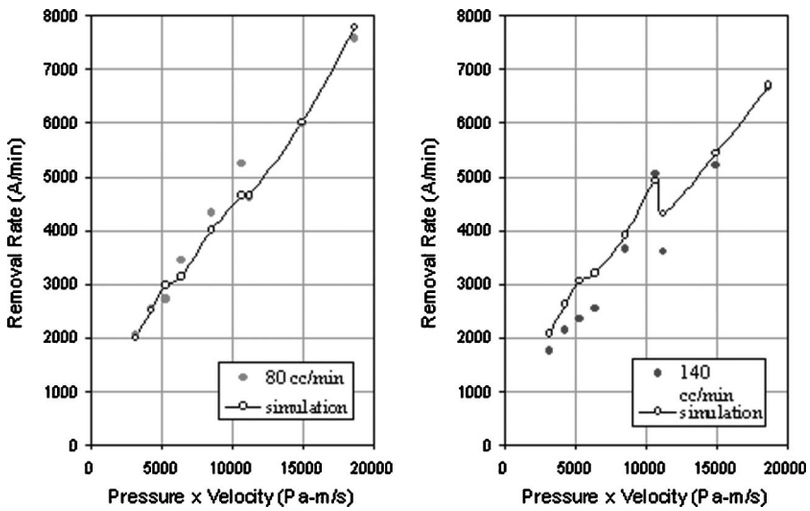


**Figure 10.** Simulation and experimental removal rate as a function of $p \times V$.

$f_s/(2\pi h_s^0 r)$, where $r$ is the radius on the pad, $f_s$ is the slurry flow rate, and $h_s^0$ is the slurry thickness between grooves. Under the wafer, it is assumed that the slurry is entrained by the pad with no outward convective motion. The slurry flow model is very rudimentary, capturing only the general outward flow. It can be seen that all other factors being equal, increasing slurry flow rate $f_s$ increases the rate at which heat is transported off the pad, resulting in cooling of the wafer due to lowering of $T_s$. In Eq. 2, the convective heat-transfer coefficient $h_{ws}$ between the wafer and slurry varies as the square root of the sliding speed. In Ref. 6, $h_{ws}$ was estimated directly from correlation theory for pad and wafer rotation rates of 120 rpm (0.93 m/s). At the same separation between the pad and wafer centers, we can relate the heat-transfer coefficient at sliding speed $V$ to the speed at 120 rpm

$$h_{ws}(V) = h_{ws}(V_{120}) \sqrt{\frac{V}{V_{120}}} \quad [3]$$

The ratio of the sliding speeds in Eq. 3 is also the same as the ratio of the rotation rates.

*Reaction rate model*.—In this report, copper removal rate can be described well by a subset of the Langmuir-Hinshelwood model in Ref. 7, summarized below. In this model, $n$ moles of an unspecified reactant $R$ in the slurry react at a rate $k_1$ with the copper film on the wafer to form a product layer $L$ on the surface

$$\mathrm{Cu} + n\mathrm{R} \xrightarrow{k_1} L \quad [4]$$

The reacted layer is then removed by mechanical abrasion with a rate $k_2$

$$L \xrightarrow{k_2} L \quad [5]$$

The abraded material $L$ is carried away by the slurry and is not redeposited. The local removal rate in this sequential mechanism is

$$RR = \frac{M_w}{\rho} \frac{k_1 C}{1 + \frac{k_1 C}{k_2}} \quad [6]$$

where $M_w$ is the molecular weight of copper, $\rho$ is the density, and $C$ is the local molar concentration of reactant. It is assumed that there is little reactant depletion so that $C$ remains constant. This allows $C$ to be absorbed into $k_1$ and be set to unity. In Eq. 6, the rate of the chemical reaction is expressed as $k_1 = A \exp(-E/kT_w)$ with $C = 1$. Assuming that the mechanical removal rate is proportional to $p \times V$, then $k_2 = c_p pV$, where $c_p$ is an assumed proportionality constant. In the mechanically limited extreme, the polish rate is $RR = (M_w c_p/\rho)pV$ and in the opposite limit it is $RR = (M_w/\rho)k_1$.

It is important to note the physical dependence of the variables in the removal rate law (Eq. 5) with this choice of $k_1$ and $k_2$. While the experimental value of $p \times V$ can be chosen at will, the local wafer temperature $T_w$ cannot because it is a function of $p \times V$ through the boundary condition expressed by Eq. 2. $T_w$ is also independently influenced by COF, $\gamma_w$, the slurry temperature, and the wafer-slurry heat-transfer coefficient, so that $p \times V$ does not completely determine the wafer temperature.

## Comparison of Theory and Experiments

The calibration of the thermal model for copper polishing and comparisons of pad temperature histories predicted by the model with measured pad temperatures, including thermal effects from *in situ* conditioning, are described in Ref. 8. This model in turn is a slight reparameterization of the same model for oxide polish.[6] In the present analysis, the important parameters involve the heat partition fraction in Eq. 1 for which the value of $\kappa_w = 217$ W/m K was chosen (*vs.* the value of 124 for silicon, and 385 for pure copper) in Ref. 8, and the wafer-slurry heat-transfer coefficient in Eq. 3, which was estimated as 762 W/m$^2$°C at 120 rpm for the application in Ref. 6. As mentioned in Eq. 1, the effective thermal conductivity of wafer was associated with the layers presented in the wafer surface. During the polishing, the wafer surface was fully or partly covered with oxide copper rather other just pure copper; thus, the effective thermal conductivity was lower than that of pure copper. The value of $\kappa_w = 217$ W/m K was an optimized one by fitting the model to the experimental measured data.

Based on this calibration, the model was run for all pressures, relative pad-wafer velocities, and slurry flow rates. The measured COF from each condition was smoothed with a linear regression line as described in Ref. 8. The ambient temperature that was employed as an initial condition in each case for the pad, wafer, and slurry and for calculating the convective heat loss to the air was estimated by averaging the five initial temperatures measured on the surface of the pad near the leading edge of the wafer. The ambient temperature was found to vary by as much as ±1.5°C about a mean of 25°C, as shown in Fig. 7a. Figure 7b compares the calculated mean pad temperature rise at sample point locations with the measured mean temperatures. These are in good agreement over all conditions, thus providing added confidence in the calibration of the model. The model then provided the wafer temperature field needed for comput-

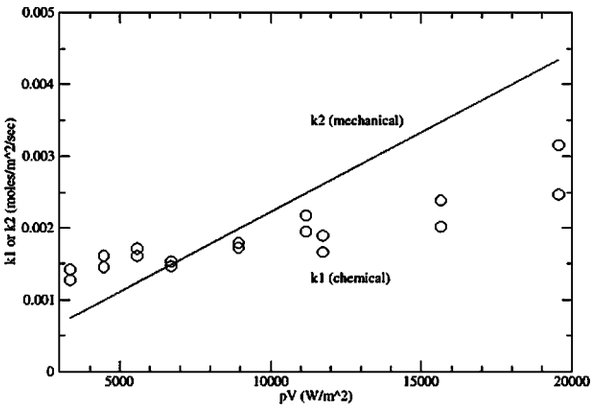


**Figure 11.** Theoretical mechanical and chemical contributions to copper removal rate.

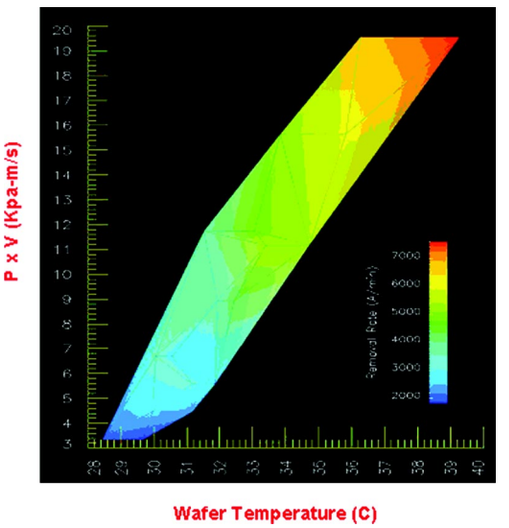


**Figure 12.** Contour graph of removal rate *vs.* wafer temperature $p \times V$.

ing the reaction rates using Eq. 6. Figure 8 shows the estimated mean wafer temperature plotted against the mean leading edge pad temperature. Results show that wafer temperature rises approximately twice as fast as the pad temperature.

Figure 9 plots the modeled and measured removal rates using the estimated mean wafer temperature rather than the mean pad temperature. Compared to Fig. 5, the removal rate data is now ''stretched'' slightly in the horizontal direction due to the temperature rescaling. It is observed that at the lower rotation rates, there is also some scatter and apparent randomization of the data points because removal rate is dependent on $1/kT$ as well as on $p \times V$.

Next, starting with the estimated mean wafer temperatures for each condition, the parameters $A$, $E$, and $c_p$ in the removal rate expression (Eq. 6) were calculated by minimizing the least-squares error between the predictions of Eq. 6 and the measured rates. The optimum values, $A = 2.7 \times 10^8$ mol/m$^2$ s, $E = 0.68$ eV, and $c_p = 2.2 \times 10^{-7}$ mol/Pa m$^3$ provided a root-mean-square (rms) fitting error of 313 Å. The estimated activation energy $E$ is close to those measured in Ref. 1 and 2. The model was then re-run under all conditions and the mean removal rate calculated over the wafer surface as shown in Fig. 10. The model reproduces much of the scatter at the lower rotation rates. As mentioned earlier, the reason for the scatter is that removal rate depends on both $T_w$ and $p \times V$ rather than just on $T_w$. The model captures the upward trend in removal rate with $p \times V$, the reduction in removal rate with increased slurry flow at higher values of $p \times V$, and the downward transition that occurs between 0.62 and 1.09 m/s.

Using the model, the underlying causes for changes in removal rate at the transition between 2.5 psi and 0.62 m/s to 1.5 psi and 1.09 m/s (at which $p \times V$ is nearly constant at 11,000 Pa m/s) were investigated. At a constant slurry flow rate of 140 cc/min, the ambient temperature, COF function, heat partition fraction, and wafer-slurry heat-transfer coefficient were systematically switched from the 1.5 psi and 1.09 m/s condition to the 2.5 psi and 0.62 m/s condition. It was found that the ambient temperature, COF, and heat partition fraction accounted for about 40% of the temperature change with the latter two accounting for most of the difference and having about equal influences. About 55% of the difference was due to a change in the convective cooling coefficient, and the remainder was accounted for by the fact that $p \times V$ was not precisely constant across the transition.

The individual values of $k_1$ and $k_2$ obtained from the fit are plotted against $p \times V$ in Fig. 11. This figure indicates that copper removal is mechanically limited at the lowest values of $p \times V$ and reaction limited at the higher values of $p \times V$. The solid line is a plot of $k_2 = c_p \times p \times V$ representing the mechanical rate constant, while circles represent the chemical rate computed by averaging $k_1 = A \times \exp(-E/kT_w)$ over the wafer surface, where $T_w$ is the wafer temperature in Kelvin. In Fig. 11, $k_2$ is represented by a straight line because it depends only on $p \times V$. The circles do not fall exactly on a straight line because $k_1$ depends on wafer temperature which is only partly determined by $p \times V$. Considering that removal rate is dependent on both thermal and mechanical factors, a contour plot describing the removal rate as the functions of temperature and $p \times V$ is a more appropriate representation of the removal rate characteristics of the copper CMP process. As shown in Fig. 12, the contour plot adequately captures the complex interplay among removal rate, temperature, and $p \times V$ during the process.

## Conclusions

Copper removal rates were examined experimentally and theoretically as a function of frictional power density and slurry flow rate under constant boundary lubrication conditions. The observed decrease in removal rate with increasing slurry flow rate was supported by theory, which attributed the change to the cooling of the wafer by the slurry. An observed transition in the removal rate that occurred when the rotation rate was changed at nearly constant value of $p \times V$ was also theoretically explained as being due to a combination of a change in the COF, the heat partition factor, and the wafer-slurry heat-transfer coefficient, with the latter being dominant. Trends in removal rates were explained as a function of $p \times V$ and the wafer temperature using a model with both chemical and mechanical components. The model was reaction rate limited at higher removal rates, emphasizing that removal of copper, unlike oxide, was in general non-Prestonian.

## Acknowledgments

The authors express their gratitude to Professor Duane Boning of MIT for allowing the authors to borrow MITs infrared camera for thermal analysis. This work was financially supported by the NSF/SRC Engineering Research Center for Environmentally Benign Semiconductor Manufacturing.

*The University of Arizona assisted in meeting the publication costs of this article.*

## References

1. J. Sorooshian, D. DeNardis, L. Charns, Z. Li, D. Boning, F. Shadman, and A. Philipossian, in *Proceedings of the 2003 CMP-MIC*, p. 43-50 (2003).
2. P. Renteln and T. Ninh, *Mater. Res. Soc. Symp. Proc.*, **566**, 155 (1999).

3. R Cowan and W. Winer, in *ASM Handbook, Friction, Lubrication and Wear Technology*, vol. 18, P. J. Blau, Editor, pp. 39-44, ASM International Materials Park, OH (1992).
4. A. Philipossian and E. Mitchell, *Micro*, **20**(7), 85 (2002).
5. Z. Li, S. Rader, P. Lefevre, K. Ina, and A. Philipossian, Paper 899 presented at The Electrochemical Society Meeting, Orlando, FL, Oct 12-17, 2003.
6. L. Borucki, L. Charns, and A. Philipossian, Paper 918 presented at The Electrochemical Society Meeting, Orlando, FL, Oct 12-17, 2003.
7. D. Thakurta, D. Schwendeman, R. Gutmann, S. Shankar, L. Jiang, and W. Gill, *Thin Solid Films*, **414**, 78 (2002).
8. L. Borucki, Z. Li, and A. Philipossian, Paper 903 presented at The Electrochemical Society Meeting, Orlando, FL, Oct 12-17, 2003.